Science Advances

AAAS

advances.sciencemag.org/cgi/content/full/3/5/e1603282/DC1

Supplementary Materials for

Evidence and mechanism of efficient thermally activated delayed fluorescence promoted by delocalized excited states

Takuya Hosokai, Hiroyuki Matsuzaki, Hajime Nakanotani, Katsumi Tokumaru, Tetsuo Tsutsui, Akihiro Furube, Keirou Nasu, Hiroko Nomura, Masayuki Yahiro, Chihaya Adachi

Published 10 May 2017, *Sci. Adv.* **3**, e1603282 (2017)
DOI: 10.1126/sciadv.1603282

This PDF file includes:

Synthesis and characterization of 2CzBN, *o*-3CzBN, and *p*-3CzBN

The emitter 2,3-di(9*H*-carbazole-9-yl)benzonitrile (**2CzBN**) was synthesized according to following procedure. Under a nitrogen atmosphere, K_2CO_3 (11.9 g, 86.3 mmol) was added to a stirred solution of 9*H*-carbazole (9.61 g, 57.5 mmol) in dry *N*-methyl-2-pyrrolidone (45 ml) at room temperature, and the mixture was allowed to react for 1 h at that temperature. Next, 2,3-difluorobenzonitrile (1.60 g, 11.5 mmol) was added, and then the mixture was stirred for 72 h at 140 °C. After cooling to room temperature, the reaction mixture was poured into a large amount of water, and the precipitate was filtered and dried in vacuum. The product was purified by silica gel column chromatography, and the product was recrystallized from methanol. The product was obtained as a white solid (yield = 2.50 g, 50.0%). ^{1}H NMR (500 MHz, $CDCl_3$) : δ=8.08-8.05 (m, 2H), 7.85 (t, J＝8.0Hz, 1H), 7.75-7.73 (m, 4H), 7.08-6.99 (m, 12H). HRMS (m/z): [M+H]+ calcd. for $C_{31}H_{19}N_3$, 433.1579; found, 433.1584.

The emitter 3,4,5-tri(9*H*-carbazole-9-yl)benzonitrile (***o*-3CzBN**) was synthesized in a fashion similar to that for **2CzBN** but using 9*H*-carbazole (3.49 g, 9.00 mmol), K_2CO_3 (4.32 g, 31.3 mmol), and 3,4,5-trifluorobenzonitrile (0.66 g, 4.17 mmol). The product was obtained as a pale yellow solid (yield = 1.51 g, 60.4%). ^{1}H NMR (500 MHz, $CDCl_3$) : δ=8.21 (s, 2H), 7.77 (dd, J＝7.5Hz, 1.0Hz, 4H), 7.36 (d, J=7.5Hz, 2H), 7.14 (d, J=8.0Hz, 4H), 7.09-7.01 (m, 8H), 6.85 (d, J=8.0Hz, 2H), 6.78 (td, J=8.0Hz, 0.5Hz, 2H), 6.63 (td, J=8.0Hz, 0.5Hz, 2H). HRMS (m/z): [M+H]+ calcd. for $C_{31}H_{19}N_3$, 598.2157; found, 598.2129.

The emitter 2,3,6-tri(9*H*-carbazole-9-yl)benzonitrile (***p*-3CzBN**) was synthesized in a fashion similar to that for **2CzBN** but using 9*H*-carbazole (20.8 g, 124 mmol), K_2CO_3 (25.7 g, 187 mmol), and 2,3,6-trifluorobenzonitrile (3.00 g, 19.1 mmol). The product was obtained as a pale yellow solid (yield = 8.11 g, 71.1%). ^{1}H NMR (500 MHz, $CDCl_3$) : δ=8.23 (d, J=9.0Hz, 1H), 8.20 (d, J＝7.5Hz, 2H), 7.99 (d, J=8.5Hz, 1H), 7.78 (dd, J=8.0Hz, 2.0Hz, 2H), 7.75 (dd, J=8.0Hz, 2.0Hz, 2H), 7.60-7.54 (m, 4H), 7.41 (td, J=8.0Hz, 1.0Hz, 2H), 7.20-7.15 (m, 4H), 7.14-7.04 (m, 8H). HRMS (m/z): [M+H]+ calcd. for $C_{31}H_{19}N_3$, 598.2157; found, 598.2147.

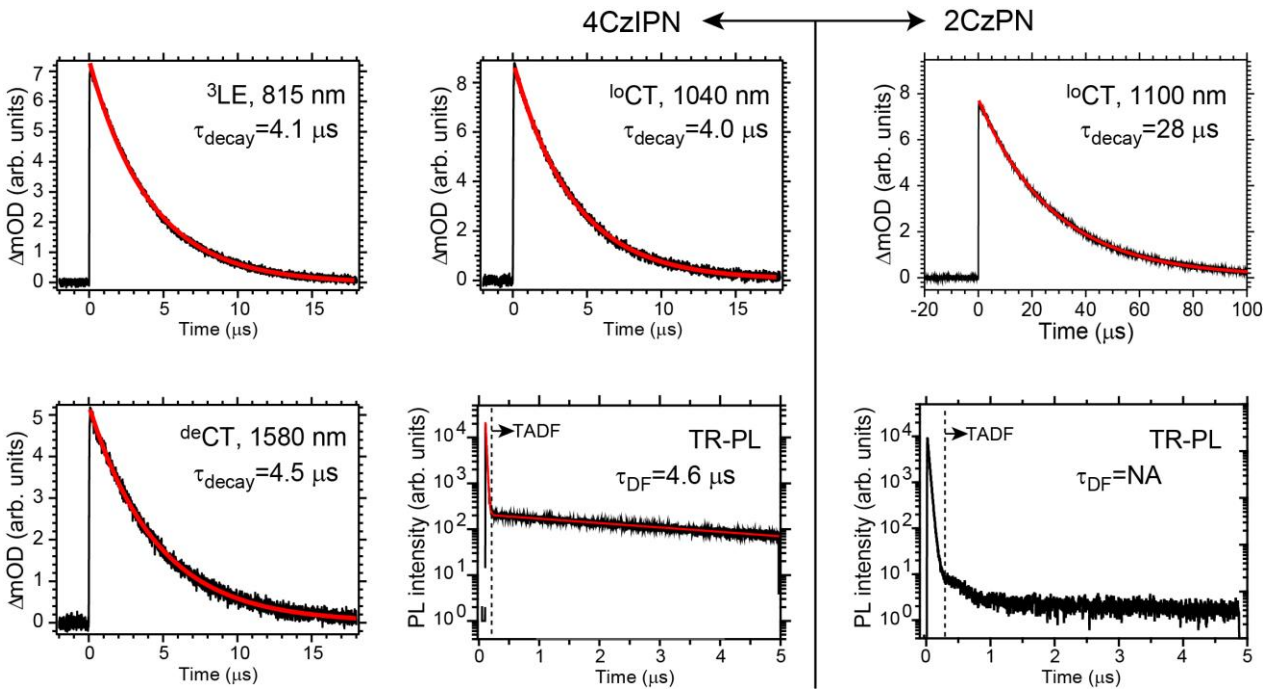

fig. S1. Time profiles of TAS of various triplet states of 4CzIPN and 2CzPN in toluene. TAS results of ^{3}LE, ^{lo}CT, and ^{de}CT and TR-PL of 4CzIPN (left) and 2CzPN (right) in toluene measured by μs-TAS technique. Black and red lines are TAS and fitting results, respectively. The curve fitting in the TAS profiles was conducted with a single exponential decay function. The τ_{decay} of each T state is included in each figure. As a reference for 4CzIPN, τ_{DF} was determined to be 4.6 μs by TR-PL measurements under N_2 gas conducted using the same procedure as in the TAS measurements. For 2CzPN, its τ_{DF} was not able to be determined owing to a limitation of the measurement time scale upto 5 μs in the set-up in AIST.

The τ_{decay} of T_1 absorptions is consisted to the τ_{DF}. This reason is theoretically described in Ref. 12. Briefly, by analysing a rate equation of TADF materials, a time-dependent population of S_1 and T_1 state is expressed by

$$S_1(t) = \frac{\lambda_{PR} - \tau_p^{-1}}{\lambda_{PR} - \lambda_{DF}} S_1(0) e^{-\lambda_{DF} t} + \frac{\tau_r^{-1} - \lambda_{DF}}{\lambda_{PR} - \lambda_{DF}} S_1(0) e^{-\lambda_{PR} t} \qquad (Singlet) \quad (1)$$

$$T_1(t) = \frac{k_{ISC}}{\lambda_{PR} - \lambda_{DF}} S_1(0) \left(e^{-\lambda_{DF} t} - e^{-\lambda_{PR} t} \right) \qquad (Triplet) \quad (2)$$

Where

$$\lambda_{PR} = \frac{1}{2} \left\{ \tau_r^{-1} + \tau_p^{-1} + \sqrt{\left(\tau_r^{-1} - \tau_p^{-1} \right)^2 + 4 k_{ISC} k_{RISC}} \right\} \qquad (3)$$

$$\lambda_{DF} = \frac{1}{2}\left\{\tau_r^{-1} + \tau_p^{-1} - \sqrt{\left(\tau_r^{-1} - \tau_p^{-1}\right)^2 + 4k_{ISC}k_{RISC}}\right\} \quad (4)$$

$$\tau_r^{-1} \equiv k_r + k_{nr} + k_{ISC} \quad (5)$$

$$\tau_p^{-1} \equiv k_p + k_{np} + k_{RISC} \quad (6)$$

where k_r and k_{nr} (or k_r and k_{np}) are the rate constant of radiative and non-radiative decay of S_1 (or T_1) state, respectively.

These equations suggest that the $T_1(t)$ also decays with a time constant of delayed fluorescence, λ_{DF}. Therefore, the time constant of decay process of T states measured by the present μs-TAS spectra virtually illustrates the time constant of TADF as depicted in Table 1.

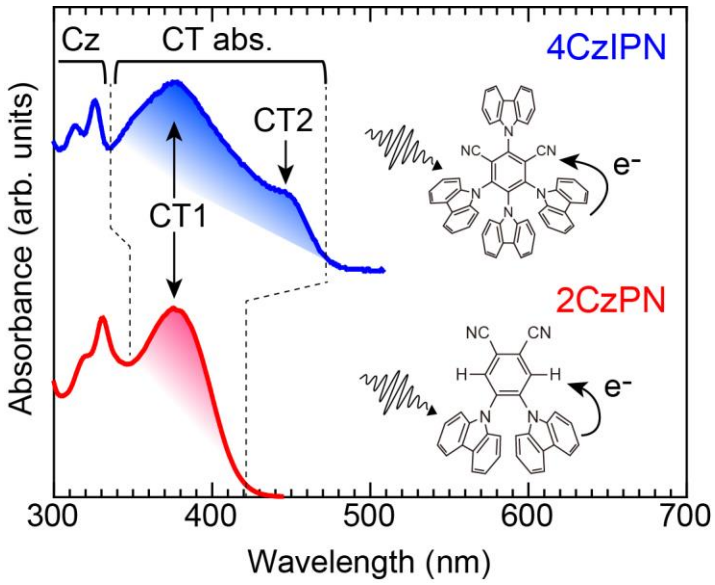

fig. S2. Steady-state absorption spectra. Ultraviolet-visible (UV-VIS) absorption of 4CzIPN (top) and 2CzPN (bottom) in toluene. The insets depict the CT from the Cz moiety to the PN core by pump light irradiation. The UV-VIS absorption spectra of 4CzIPN and 2CzPN show absorption features longer than the local excitation of Cz moieties. The features are ascribed to intramolecular CT absorption of each molecules (5). Theoretical molecular orbital calculations supports this assignment because the highest occupied molecular orbitals (HOMOs) and the lowest unoccupied MOs (LUMOs) are localized on the Cz moieties and PN core, respectively. Therefore, the pump lasers used for TAS measurements, 355 or 400 nm, directly excite the CT transitions of 4CzIPN and 2CzPN, which produces an intramolecular charge-separation between the Cz moieties and PN core. Thereby, the probe lights used for fs-, ns-, and μs-TAS measurements directly reflect the excited-state after this CT transition of both molecules occured.

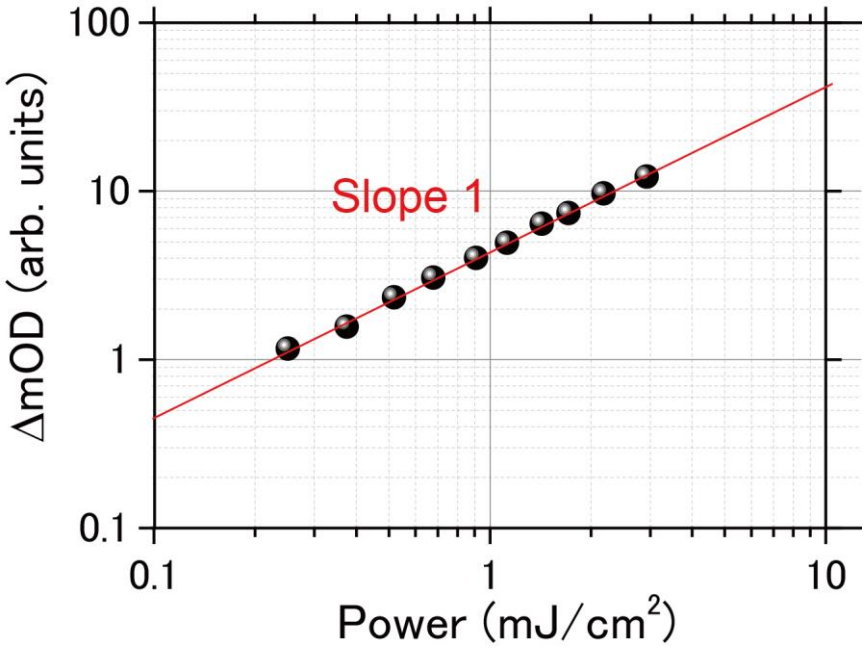

fig. S3. Laser power dependence in TAS spectra. ΔOD at an adsorption wavelength of Cz^+ (860 nm) of 4CzIPN in toluene solution (concentration: 3 x 10^{-5} mol/L) as a function of pump laser power. The data was taken at Δt = 1 ns measured in ns-TAS spectra. The ΔOD increases proportional to the irradiated power of pump light source. This indicates that the second-order reaction is ignored in the present measurements and a first-order reaction (i.e., intramolecular CT) is dominant one.

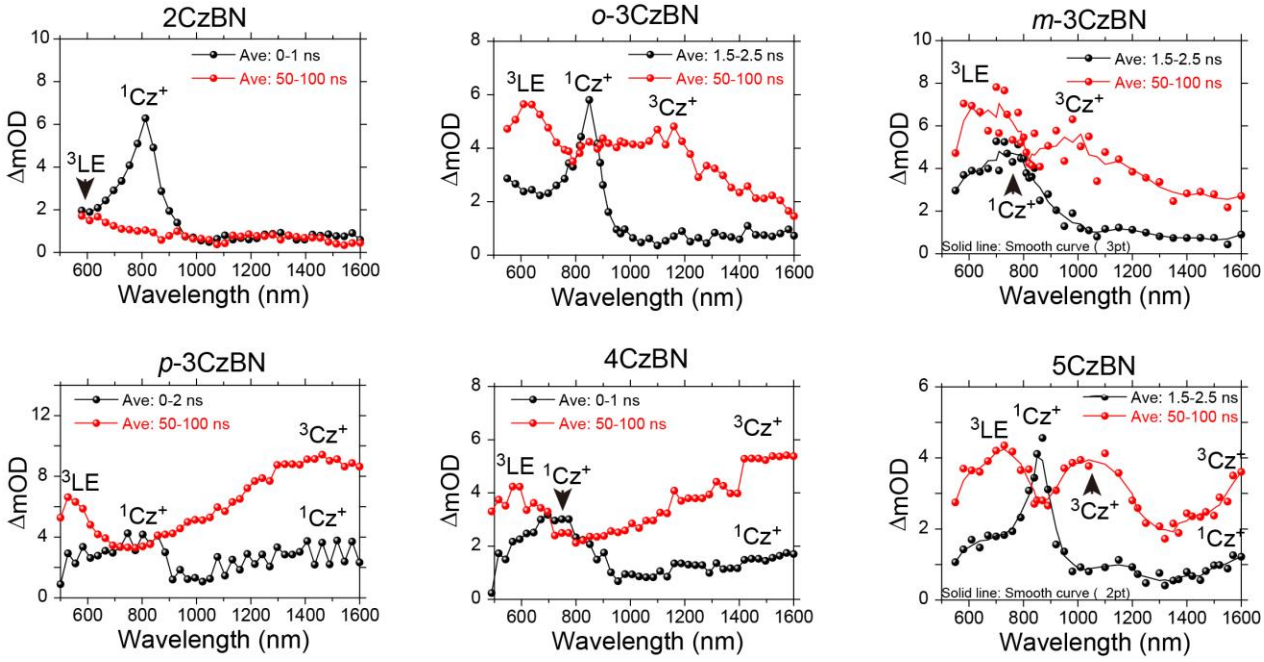

fig. S4. TAS spectra of the CzBN derivatives. The TAS spectra at Δt below or above τ_{prompt} of the CzBN derivatives. The corresponding τ_{prompt} are shown in Table 1 in the main manuscript.

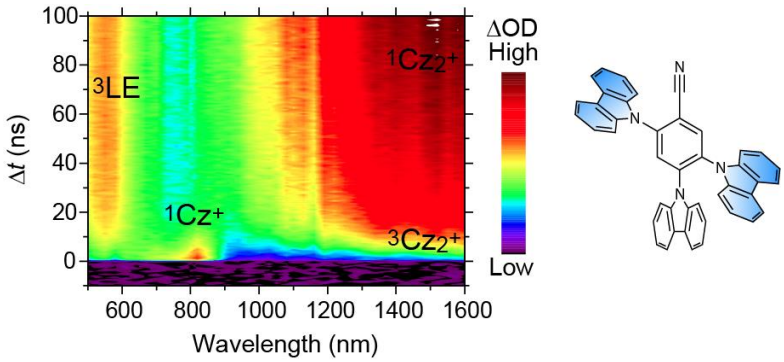

fig. S5. TAS results of 3, 4, 6-*p*-3CzBN. A contour map of ns-TAS results of 3, 4, 6-*p*-3CzBN in toluene solution (concentration: 6.7 x 10^{-5} mol/L). Pump laser power is 1.14 mJ/cm^2.

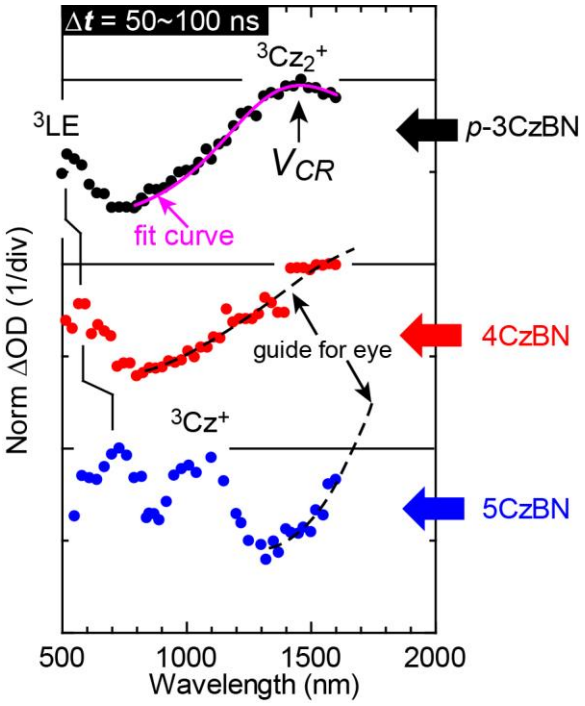

fig. S6. Energy position of CR band. A comparison of the TAS spectra in the T state of *p*-3CzBN, 4CzBN, and 5CzBN. The curve fitting (pink) of CR band ($^3Cz_2^+$) was done using a single Gauss function. V_{CR} was observed clearly for 2CzBN at 1460 nm and was shifted towards longer and longer wavelengths in the order of 4CzBN and 5CzBN (see the broken lines overlapped on the CR band).

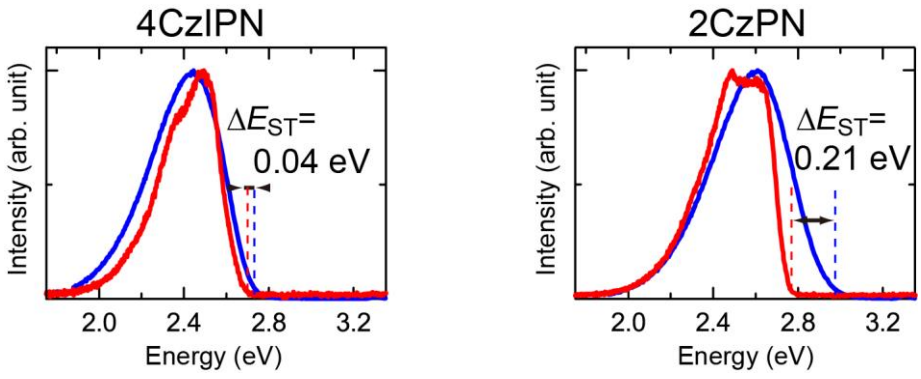

fig. S7. Emission spectra of CzPN derivatives. The fluorescence and phosphorescence spectra (77 K) of 4CzIPN (left) and 2CzPN (right) in toluene solution. The ΔE_{ST} in each figures is estimated from threshold energy of the fluorescence and phosphorescence spectra, as in CzBN derivatives in Fig. 2B. Note that the ΔE_{ST} of 4CzIPN in the left figure differs from the activation energy of 5±1wt%-4CzIPN doped-CBP films, 0.083 meV, reported in Ref. (*5*).

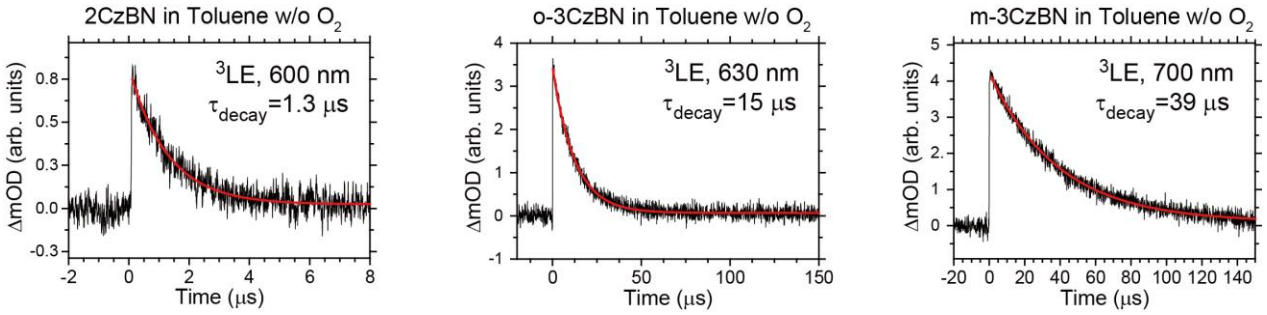

fig. S8. Time profiles of TAS of triplet states of CzBN derivatives. TAS results of ^{3}LE of 2CzBN, *o*-3CzBN, *m*-3CzBN in toluene measured by μs-TAS. Black and red lines are the TAS and fitting results, respectively. The curve fitting was conducted with a single exponential decay function. The τ_{decay} of each profiles is included in each figure.